Journal of Power Sources 196 (2011) 508–513

Contents lists available at ScienceDirect

Journal of Power Sources

journal homepage: www.elsevier.com/locate/jpowsour

An investigation of zincite from spent anodic portions of alkaline batteries: An industrial mineral approach for evaluating stock material for recycling potential

Heather A. Barrett[a], Olaf Borkiewicz[b], Mark P.S. Krekeler[a,*]

[a] Department of Geology, Miami University Hamilton, 1601 University Blvd., Hamilton, OH 45011, United States
[b] Department of Geology, 501 East High St., Miami University, Oxford, OH 45056, United States

ARTICLE INFO

Article history:
Received 20 June 2010
Received in revised form 5 July 2010
Accepted 6 July 2010
Available online 13 July 2010

Keywords:
Zincite
Transmission electron microscopy
Scanning electron microscopy
Spent alkaline battery recycling
Anodic material

ABSTRACT

The mineralogy of anodic portions of spent alkaline batteries from a leading brand (Duracell) that had been equilibrated in ambient air for approximately 4 months was investigated to determine if material generated from this low energy process may be suitable stock material for recycling. Powder X-ray diffraction (XRD) identified the bulk of the ambient air oxidized anodic material as zincite (ZnO). Scanning electron microscopy investigation indicates a variety of textures of zincite are present with euhedral hexagonal prisms being the most common crystal form. Energy dispersive spectroscopy (EDS) analysis indicates that there are no minor amounts of Mn within the zincite. Transmission electron microscopy investigation indicates a variety of textures exist in the <2 μm size fraction including near euhedral prismatic crystals, crystals with step-fashion terminations and indentations, heavily corroded zincite and near amorphous aggregates of anastomozing zinc oxide. Impurities in the <2 μm size fraction include minor amounts of unidentified mixed sulfate materials and are interpreted as dominantly occurring as thin coatings on zincite particles. Discrete submicrometer-sized spherical and rhomboid particles of Zn–Mn oxides are also common impurities in the <2 μm size fraction but occurr at abundance of <1% by volume.

This study provides new baseline information that can be used to develop large scale recycling of zincite from spent alkaline batteries. A promising applications of zincite are numerous, including the development of new solar cell materials. The spent alkaline battery waste stream may serve as promising resource for driving further development of this sector of the economy.

1. Introduction

According to the USEPA U.S. citizens use an average of eight disposable alkaline batteries per year. With a population of approximately 300 million people, this translates into an estimated 2.4 billion batteries used and disposed of each year. It is well recognized that other battery technologies have established recycling mechanisms [1–8]. However, disposable alkaline batteries are not yet commonly recycled globally. There are methods for recycling alkaline batteries [9–16]. These processes are usually very energy or material intensive, do not meet environmental needs and often are not profitable. For example some processes entail cryogenic dismantling followed by drying, grinding, screening, leaching with H_2SO_4, which is then followed by a liquid–liquid extraction [13]. Other processes are heat intensive and involve firing to 105 °C and also to 650 °C for several hours, use of EDTA, acetic acid and sulfuric acid [14]. Both of these examples have significant environmental detractions and neither produce high value materials.

Disposable alkaline batteries consist of two fundamental modular parts, an anodic region and a cathodic region which are separated by a permeable membrane. The anodic region contains un-reacted metallic zinc, typically a KOH solution, some gelling agents, and ionic zinc which accumulates during discharge of the battery. The cathodic region is composed of electrolytic manganese dioxide (EMD) and is reported to consist of MnO_2 (such as ramsdellite) and other manganese oxide or oxyhydroxide compounds including but not limited to Mn_2O_3, MnO and $Mn(OH)_2$ as well as aqueous zinc ions [14,15]. Other investigations have investigated the phase composition of EMD using Rietveld refinement techniques and transmission electron microscopy and found that γ-MnO_2 and ε-MnO_2 forms dominate with lesser amounts of β-MnO_2 occuring [16]. Accordingly, these materials are a major waste stream globally [17,18] and can be a significant contributor to heavy metals in landfills [18,19].

Improvements in the recycling of alkaline batteries are clearly needed to make the processes more agreeable with pollution prevention protocols and more profitable. Low energy and low material consuming processes need to be developed to augment the overall recycling of alkaline batteries. Furthermore if materials derived from the recycling of disposable alkaline batteries

* Corresponding author. Tel.: +1 513 785 3106; fax: +1 513 785 3145.
E-mail address: krekelmp@muohio.edu (M.P.S. Krekeler).

0378-7753/$ – see front matter © 2010 Elsevier B.V. All rights reserved.
doi:10.1016/j.jpowsour.2010.07.013

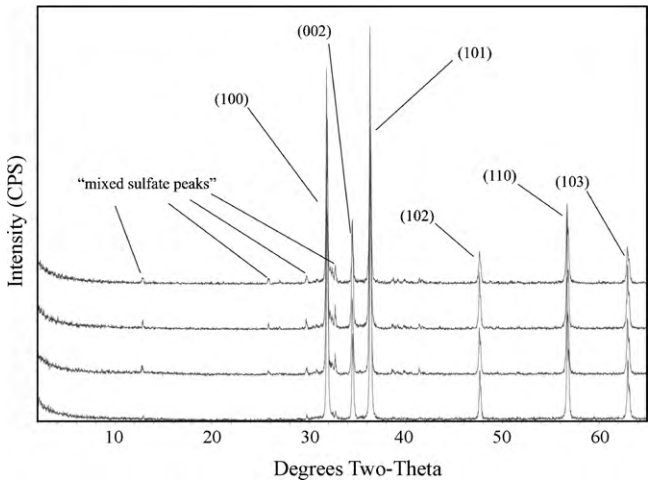

Fig. 1. Representative X-ray diffraction patterns of ambient air oxidized spent anodic portions of Duracell batteries. Miller indices of respective peaks of zincite are labeled as are peaks tentatively identified as "mixed sulfate".

have environmental benefits, this should help drive recycling efforts.

Zincite is a waste product derived from the anodic portion of spent alkaline batteries and there are no detailed studies of this waste material. From an applied materials perspective, zincite is an important semiconductor material that has gained a great deal of attention over the past decade. This material has a wide band gap of 3.37 eV and also a large exciton binding energy of 60 meV, producing excitonic survival above room temperature. These properties make zincite suitable for a broad range of uses and numerous applications exist for zincite including optical switches [20,21], light emitting diodes [22] and solar cells [23–25]. Typical synthesis procedures for zincite nanoparticles involve calcining zinc acetate ($Zn(CH_3COO)_2{\cdot}H_2O$) at 800 °C. However low temperature aqueous routes involving several substrates are now known but heating to 60–80 °C is still required [26].

The nature of zincite from battery waste is largely unknown and investigations are required if recycling of this material is to occur. Size, morphology, and crystallinity of the zincite particles as well as the nature of impurities must be constrained. Whether or not low temperature recycling approaches produce viable materials is unknown. Zincite from ambient air oxidation of anodic portions of a leading brand of disposable alkaline batteries was investigated to assess if this low energy, low chemical intensive approach could yield potentially viable stock material for recycling.

2. Materials and methods

All sample preparation and analytical work was carried out at Miami University. Anodic portions of Duracell size "D" alkaline batteries were extracted by cutting the battery body perpendicular to the length at the negative end with a Dremel tool utilizing a carborundum grinding wheel. The anodic portions were extracted after gently separating the cathodic region with a flat edged tool or gently crushing the battery to fracture the cathodic region. Upon removal, the anodic portion was contained in the cell membrane and was allowed to dry in ambient air. This raw material sat in ambient air in an enclosed hood for approximately 4 months. This was done to simulate accumulation of material from a recycling stream and ensure equilibrium with the atmosphere. The colors of each sample were then compared to the Munsell color chart for comparison and the colors observed were within the neutral range of gley 1, 7/8, and within the range of gley 2 8/5PB and 8/10B.

Carbon adhesive tabs were used to mount the samples on aluminum stubs using clean forceps. SEM investigation was done with variable pressure field emission scanning electron microscope (FESEM, Zeiss Supra 35VP FEG) using nitrogen (N_2) as the compensating gas. The instrument is equipped with an energy dispersive spectrometry (EDS) detector EDAX2000 and has a detection limit of approximately 0.1 wt% for most elements.

For transmission electron microscopy (TEM), the <2 μm size fraction from deionized water suspensions was investigated from

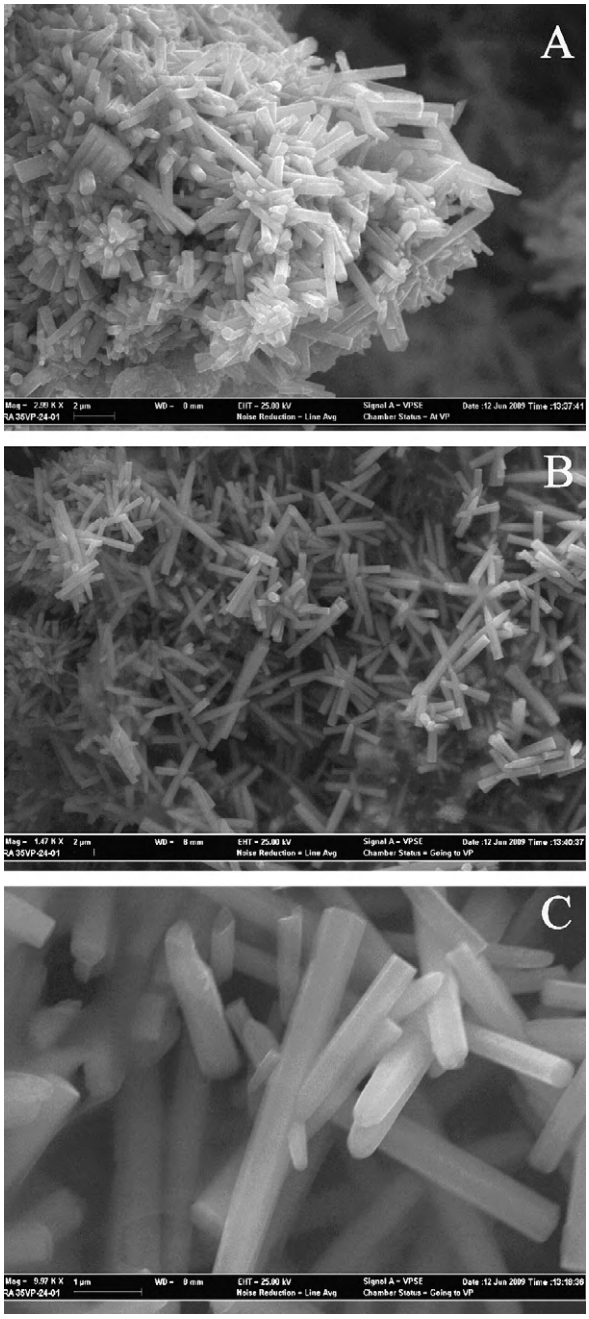

Fig. 2. Representative SEM images showing the morphology of zincite crystals. (A) SEM image at approximately 3000× showing nearly spherical to ovoid shape aggregates of radial euhedral crystals of zincite. (B) A slightly lower magnification (approximately 1500×) SEM image showing euhedral hexagonal prisms of zincite which are the dominant texture in the samples. (C) A slightly higher magnification (approximately 10,000×) SEM image showing some euhedral hexagonal prisms with apical terminations.

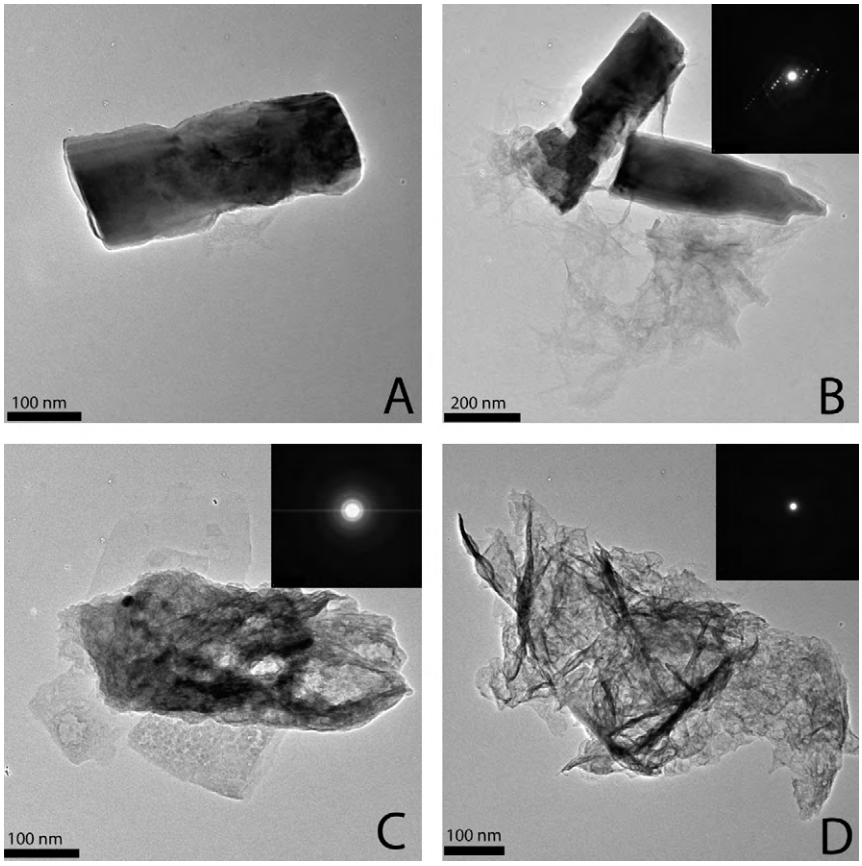

Fig. 3. Representative bright field TEM images showing the range of particle morphologies of zincite in the <2.0 μm size fraction. (A) An example of the common near euhedral prismatic zincite crystals. (B) An example of less common zincite crystals with step-fashion terminations and indentations. Inset SAED pattern is from the upper grain and indicates the particle is a single crystal. (C) An example of a heavily corroded zincite particle. The inset SAED has significant streaking indicating poor crystallinity of the particle. (D) Near amorphous aggregates of anastomozing zinc oxide material. The SAED pattern has no diffraction spots.

an unwashed separate and a separate that had been washed with deionized water repeatedly until the pH of the supernatant was approximately 7.0 which required a water to solids ratio of approximately 24:1 to 32:1. TEM grain mounts were prepared by placing a drop of the suspension on 3 mm Cu grids with Formvar film. Bright field imaging was carried out using a JEOL JEM-2100 transmission electron microscope fitted with a Bruker Silicon drift XEDS detector. The instrument was operated at 200 kV with a beam current of 106 μA. All images were acquired with a Gatan OriusTM SC 200D CCD camera with a 2048 × 2048 pixel resolution.

For powder X-ray diffraction, sample material was gently ground by hand in an agate mortar and pestle. Powder X-ray diffraction data was collected using a Scintag X-1 powder diffractometer equipped with a Peltier detector, using Cu Kα2 (0.1548 nm) radiation operating at 40 kV and 35 mA. Samples were scanned from 5° to 65° 2θ at 0.02° steps using a count time of 1 s per step. Phase identification was determined using the computer program Jade and PDF card 036-1451 for zincite.

3. Results

Powder XRD results show that the samples are dominated by zincite with the major diffraction peaks of (1 0 0), (0 0 2), (1 0 1), (1 0 2), (1 1 0), and (1 0 3) being detected in all samples (Fig. 1). Other crystalline materials were present in the samples, however these peaks were an order of magnitude or more less intense. Peaks with *d*-spacing values of approximately 0.690 nm, 0.345 nm, 0.300 nm and 0.275 nm are common, however these peaks cannot be indexed and the phases could not be confidently identified. Because sulfuric acid, potassium hydroxide, and aqueous zinc and manganese are all probable components of the electrolyte phase of spent disposable alkaline batteries, we tentatively identify these peaks as "mixed sulfate".

SEM investigation of samples indicates that radial aggregates of zincite crystals are very common and are the dominant texture (Fig. 2). Aggregates are commonly 2–10 μm in diameter and have a nearly spherical to ovoid shape. Individual crystals are usually euhedral hexagonal prisms that vary in length from approximately 0.3 to 5 μm and vary in width from approximately 0.1 to 0.8 μm. Approximately 95% or more of prisms are terminated by flat euhedral (0 0 1) faces and remaining terminations are apical in nature. EDS analyses of zincite crystals suggest they are pure, however minor K and S peaks are common and are interpreted as part of the "mixed sulfate" which may coat exteriors of crystals. No discrete sulfate crystals were observed.

TEM study indicates a variety of textures exist in the <2 μm size fraction (Fig. 3). Near euhedral prismatic zincite crystals are dominant with dimensions varying from approximately 100 nm × 300 nm to 200 nm × 600 nm. Selected area electron diffraction (SAED) patterns from these particles indicate that they are single crystals. These particles constitute approximately 90% of the population of sample material in the <2 μm size fraction. Subeuhedral zincite crystals with irregularities such as step-fashion terminations and indentations are less common and comprise an estimated 2–3% of the sample material. Other textures exist in less abundance that indicate progressive corrosion. Poorly crystalline anhedral zincite crystals that are adhered to

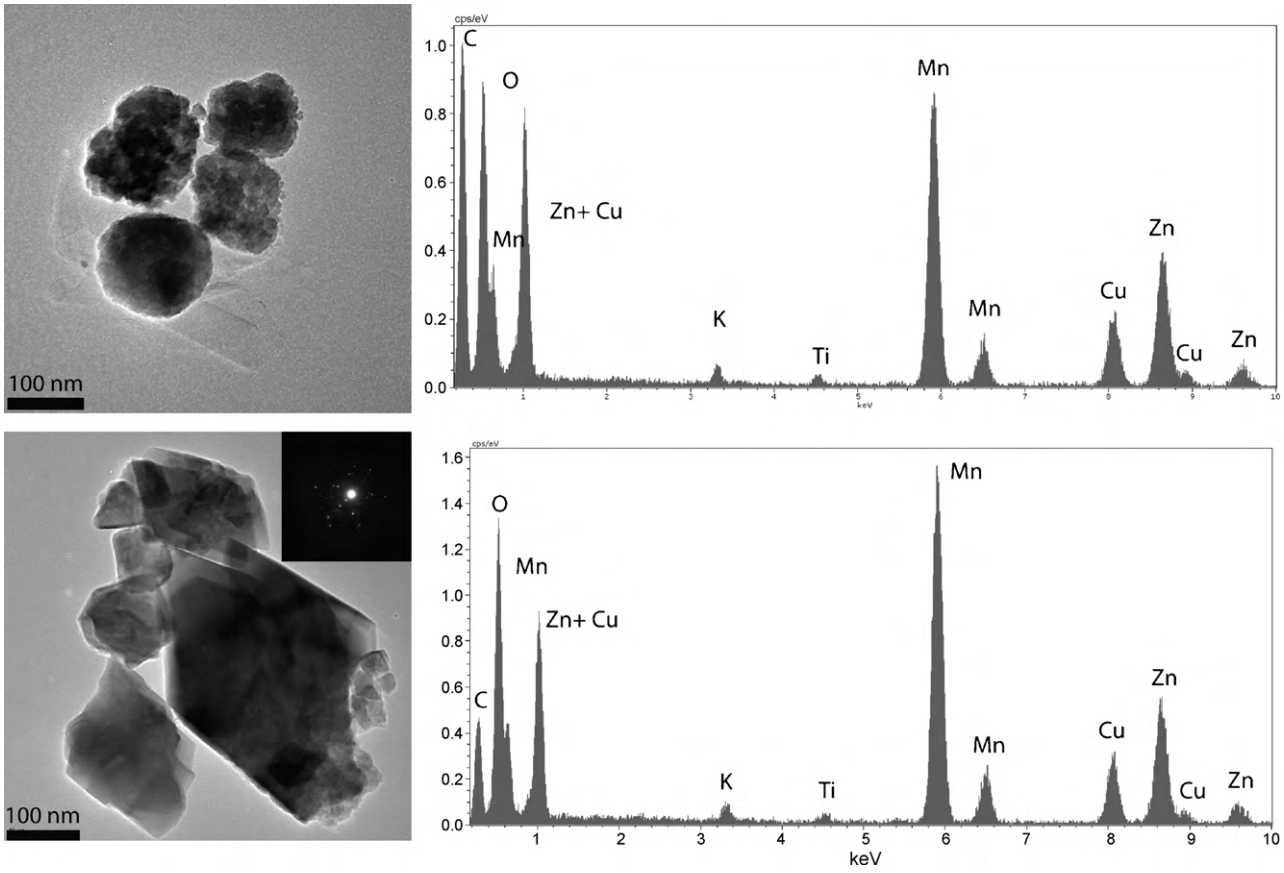

Fig. 4. Representative bright field TEM images showing Zn–Mn oxides as spherical aggregate and rhomboid particle impurities with respective EDS spectra adjacent to each. Cu lines are interpreted to originate from the sample grid whereas Ti is interpreted as integral to the particles.

amorphous K-rich particles were commonly observed and comprised approximately 1–2% of the sample material. SAED patterns from this material are heavily streaked. Nearly amorphous aggregates of anastomozing zinc oxide-rich material are also common and have SAED patterns with no diffraction spots. Potassium-rich amorphous particles are commonly associated with these zinc oxides.

Two textures of Zn–Mn oxides are observed as well in the <2 μm size fraction and collectively these textures comprise an estimated <1% of the sample (Fig. 4). A spherical aggregate texture and a rhomboid texture are observed. Spherical textures are nearly uniform and are approximately 100 nm in diameter. Rhomboid particles are more varied in morphology being subhedral to euhedral with diameters approximately 100–400 nm. Both spherical aggregates and rhomboid particles have similar chemical compositions having large quantities of O, Mn, Zn, and lesser quantities of K and Ti.

An aqueous mixture of Zn powder, zincite and dried battery electrolyte solution (KOH) is expected to have a high pH and no doubt will determine the nature of the materials used in the handling and equipment to be utilized in the recycling process. As an assessment for suitability for water processing, sample material was mixed with deionized water at a concentration of approximately 1:15. The initial pH readings varied between 9.3 and 9.53, the temperatures ranged between 23.3 °C and 23.5 °C, and the oxidation reduction potential (ORP) spanned from −129.1 mV to −149.0 mV. When the measurements were taken again, 2 weeks later and after submersion in an ultrasonic bath, the pH varied from 8.31 to 8.73, the temperature varied from 24.4 °C to 25.3 °C, and the ORP varied from −79.4 mV to −101.4 mV.

4. Discussion

Ambient atmospheric oxidation over a period of 4 months produces a consistently uniform mineralogy dominantly of zincite and much lesser amounts of an unidentified “mixed sulfate”. Powder X-ray patterns of material are very similar in both peak position and intensity of both phases. Discrete crystals of metallic zinc were not observed suggesting a high yield of zinc powder to zincite conversion of 99+%.

Although there is clear potential for recycling spent anode material, several challenges exist in the development of products or applications of high quality from stock material generated by this ambient air oxidation process. One challenge is the removal of impurities. A wash process is likely needed to remove excess KOH, “mixed sulfate” or electrolyte solutions adhered to the surface of zincite particles. Small quantities of Zn–Mn oxides occur in the zincite powder as impurities. Compositions and textures of these Zn–Mn oxides particles are consistent with hetaerolite which is a common component of some spent batteries. For applications requiring high purity these can be problematic. For simple applications such as paint pigment these impurities may be less problematic. A significant difference in density between zincite ($d = 5.67$) and hetaerolite ($d = 5.25$) exists and a water separation process such as batch washing followed by centrifuge that exploits particle size and density may be an effective strategy for purification. Particle size distribution and shape is somewhat variable. Euhedral prismatic zincite particles are dominantly micrometer-sized and should be easily separated by centrifuge. Most of the irregularly shaped crystalline zincite particles, amorphous zincite particles,

and Zn–Mn oxide impurities are submicrometer (<600 nm) in size.

Zincite produced by the ambient air oxidation process does not yield nanoparticle size distributions. Crystal growth of ZnO nanoparticles has been observed in ambient atmosphere conditions and the mechanism of this process is thought to be related to humidity in the air driving the reaction [27]. Controlling the atmospheric composition of the ambient oxidation process may induce smaller particle size distributions and thus may potentially yield higher value materials and merits further investigation.

Investigations of solid solution behavior in ZnO are largely conducted at high temperatures. Investigations commonly involve iron [28], copper [29,30], cobalt [31] and more complex systems involving Mg and Fe [32] and Al and Fe [33]. High temperature investigations of ZnO–MnO solid solution are uncommon. Limited investigation of solid-state interactions between wurtzite and manganese oxides in air using diffusion coupling techniques have been conducted [34]. No diffusion was observed at temperatures below 973 K. Above this temperature, Mn(IV) is reduced to Mn(III) and the subsequent formation of Mn_2O_3 drives the diffusion of manganese into the ZnO material, yet it never enters the wurtzite lattice and accordingly, no homogeneous MnO:ZnO solid solution is formed. Zn however greatly diffuses in the manganese oxide pellet, and a new phase layer of cubic and tetragonal spinel-type phases initially develops at the interface region. Differences arising between ZnO, MnO_2 and Mn_2O_3 crystal structures are interpreted as the cause of variation of diffusion behaviors.

Zincite does form in natural high temperature geologic environments, primarily at Franklin and Sterling Hill, New Jersey. These are settings where Mn is a major component of the environment and in these natural geologic settings the substitution of Mn in the zincite structure is possible [35,36]. Despite the association of the metallic zinc powders with Mn in the spent alkaline batteries, no such substitution was observed above the detection limit (approximately 0.1 wt%) of the EDS analyses of zincite particles in either SEM or TEM investigation.

The general approach outlined in this paper broadly follows the USEPA's P^3 design guidelines as the approach involves reuse of a waste stream, low energy consumption, and no need for additional chemicals. The process is not free of environmental and safety concerns as water used in processing will need to be recycled. Handling the zincite in aqueous suspension in a process stream will require some degree of corrosion resistant piping and materials owing to the reasonably high pH range observed. The current particle size distribution however should pose no major safety concerns requiring anything beyond normal personal protection protocols.

This study provides new baseline information that can be used to develop process streams for large scale recycling of zincite from spent alkaline batteries. Further work to constrain the identification of the mixed sulfate phases is needed and likely requires use of a humidity control chamber. The next phase of development includes applying industrial mineral processing techniques to purify the zincite. Similar approaches for recycling the manganese oxide-rich cathodic regions of spent alkaline batteries have been proposed [37].

Potential applications of zincite are numerous [38]. Of particular concern for power sources is the use of zincite in solar cells [39–41]. Although zincite based solar cells show much promise the economic feasibility of using these materials is currently low considering current x–Si based cells and less conventional materials such as FeS_2, CuO, and Zn_3P_2 [41]. The spent alkaline battery waste stream may serve as promising resource for driving further development of zincite applications in the solar cell sector of the economy.

5. Conclusions

This is the first detailed industrial mineralogical investigation of anodic material from spent alkaline batteries. The ambient air oxidation approach can produce stock zincite material which can be refined and reprocessed. The results of this study suggest that anodic materials may have a mineralogical composition consistent with the needs for recycling a range of materials, including pigments and near nanoparticle size applications. Further work on the assessment of applicability of refined zincite particles for the numerous product types is required. It is expected that the simple ambient air oxidation approach could be modified in numerous ways to control crystal morphology and size.

Acknowledgements

We thank Duracell Corporation for valuable discussion and two anonymous reviewers for valuable comments. Work was partially supported by a start up grant to Krekeler from Miami University-Hamilton. We thank Dr. Richard Edelman and Mr. Matt Duley of Miami University's electron microscopy facility for general assistance. Transmission electron microscopy investigation was supported by National Science Foundation grant EAR 0722807 to Miami University.

References

[1] D.P. Mantuano, G. Dorella, R.C.A. Elias, M.B. Mansur, J. Power Sources 159 (2006) 1510.
[2] H. Roberts, J. Power Sources 116 (2003) 23.
[3] A. Zabaniotou, E. Kouskoumvekaki, D. Sanopoulos, Resour. Conserv. Recy. 25 (1999) (1999) 301.
[4] A.G. Morachevskii, Russ. J. Appl. Chem. 70 (1997) 1.
[5] G. Diaz, D. Andrews, J. Miner. Metal. Mater. Soc. 48 (1996) 29.
[6] P. Ammann, J. Power Sources 57 (1995) 41.
[7] S. Frohlich, D. Sewing, J. Power Sources 57 (1995) 27.
[8] C. Sancilio, J. Power Sources 57 (1995).
[9] G.X. Xi, L. Yang, M.X. Lu, Mater. Lett. 60 (2006) 3582.
[10] J.M. Nan, D.M. Han, M. Cui, M.J. Yang, L.M. Pan, J. Hazard. Mater. 133 (2006) 257.
[11] M.B.J.G. Freitas, M.K. de Pietre, J. Power Sources 143 (2005) 270.
[12] Y.Q. Xia, G.J. Li, Waste Manage. 24 (2004) 359.
[13] A.L. Salgado, A.M.O. Veloso, D.D. Pereira, G.S. Gontijo, A. Salum, M.B. Mansur, J. Power Sources 115 (2003) 367.
[14] N. Vatistas, M. Bartolozzi, S. Arras, J. Power Sources 101 (2001) 182.
[15] N. Vatistas, M. Bartolozzi, J. Power Sources 79 (1999) 199.
[16] D.E. Simon, R.W. Morton, J.J. Gislason, Adv. X-ray Anal. 47 (2004) 267.
[17] R.J. Slack, J. Gronow, N. Voulvoulis, Sci. Total Environ. 337 (2005) 119.
[18] S. Panero, C. Romoli, M. Achilli, E. Cardarelli, J. Power Sources 57 (1995) 9.
[19] J. Avraamides, G. Senanayake, R. Clegg, J. Power Sources 159 (2006) 1488.
[20] H. Lin, Appl. Phys. Lett. 90 (2007), UNSP 223110.
[21] H. Kind, H.Q. Yan, B. Messer, M. Law, P.D. Yang, Adv. Mater. 14 (2002) 158.
[22] H. Kim, J.S. Horwitz, W.H. Kim, J.A. Mäkinen, Z.H. Kafafi, D.B. Chrisey, Thin Solid Films 420 (2002) 39.
[23] S.H. Eom, S. Sentbilarasy, P. Uthirakumar, C.H. Hong, Y.S. Lee, J. Lim, S.C. Yoon, S.H. Lee, Sol. Energ. Mater. Sol. Cell 95 (2008) 564.
[24] J.B. Baxter, E.S. Aydil, Appl. Phys. Lett. 86 (2005) 0531144.
[25] A.B. Kashyout, M. Soliman, M. El Gamal, M. Fathy, Mater. Chem. Phys. 90 (2005) 230.
[26] R. Habibi, J.T. Daryan, A.M. Rashidi, J. Exp. Nanosci. 4 (2009) 35.
[27] M. Ali, M. Winterer, Chem. Mater. 22 (2010) 85.
[28] T. Yamashita, R. Hansson, P.C. Hayes, J., Mater. Sci. 41 (2006) 5559.
[29] J. Cernak, F. Gerard, C. Kappenstein, J. Chomic, Monatsh. Chem. 135 (2004) 1081.
[30] P. Porta, S. Derossi, G. Ferraris, F. Pompa, Solid State Ionics 45 (1991) 35.
[31] L. Poul, S. Ammar, N. Jouini, F. Fievet, F. Villain, Solid State Sci. 3 (2001) 31.
[32] R. Hansson, P.C. Hayes, E. Jak, Scand. J. Metall. 33 (2004) 355.
[33] R. Hansson, P.C. Hayes, E. Jak, Metall. Mater. Trans. B 35 (2004) 633.
[34] M. Peiteado, A.C. Caballero, D. Makovec, J. Solid State Chem. 180 (2007) 2459.
[35] E.P. Henderson, Gems Gemol. 5 (1945) 251.

[36] C. Klein, Hurlbut, Manual of Mineralogy, after J.D. Dana, 20th edition, 1985, 596 p.
[37] M.P.S. Krekeler, Waste Manage. 28 (2008) 2061.
[38] U. Özgür, Y.A. Alivov, C. Liu, A. Teke, M.A. Reshchikov, S. Doğan, S. Avrutin, S.J. Cho, H. Morkoç, J. Appl. Phys. 98 (2005) 041301.
[39] A.K. Das, P. Misra, L.M. Kukreja, J. Phys. D: Appl. Phys. 42 (2009) 165405.
[40] X. Wang, Q. Lei, W. Xu, W. Zhou, J. Yu, Mater. Lett. 63 (2009) 1371.
[41] C. Wadia, A.P. Alivisatos, D.M. Kammen, Environ. Sci. Technol. 43 (2009) 2072.